

Electronic Supplementary Information

Palladium-mediated radical homo-coupling reactions: a surface catalytic insight

Isabelle Favier,^a Marie-Lou Toro,^a Pierre Lecante,^b Daniel Pla,^{*a} and Montserrat Gómez^{*a}

^a Laboratoire Hétérochimie Fondamentale et Appliquée (LHFA), Université de Toulouse 3 – Paul Sabatier and

CNRS UMR 5069, 118 route de Narbonne, 31062 Toulouse Cedex 9, France.

^b Centre d'Elaboration de Matériaux et d'Etudes Structurales (CEMES), CNRS UPR 8011, 29 rue J. Marvig, 31055

Toulouse, France

TABLE OF CONTENTS

A. Materials and Instrumentation, General Experimental Procedures	S2-S4
B. Characterization of preformed palladium nanoparticles, PdXNPs (Figs. S1 – S3)	S5-S6
C. Reaction Optimization Studies (Table S1)	S7
D. TEM analysis after catalysis (Fig. S4)	S8
E. TEM analysis of Pd/C dispersed in glycerol (Fig. S5)	S8
F. Halide effect studies (Table S2)	S9
G. Determination of bromine content by X-ray fluorescence measurements	S10
H. Mechanistic insights for the homo-coupling reaction (Figs. S6 et S7)	S11-S12
I. Characterization of bis-aryls 4 , 6-8 , 10 , 11 , 13	S13-S16
J. ¹ H, ¹³ C, and ¹⁹ F NMR Spectra of Selected Compounds 4 , 6-8 , 10 , 11 , 13	S17-S23
K. References	S24

A. General Experimental Procedures, Materials and Instrumentation.

Instrumentation. Automated flash chromatography was performed with an Isco Teledyne Combiflash medium-pressure liquid chromatograph with prepacked C18 (15 μm) or silica gel (47-60 μm) columns. NMR spectra were recorded on a Bruker Advance 300 spectrometer at 293 K (300 MHz for ^1H NMR and 75.4 MHz for ^{13}C NMR). Chemical shifts (δ) are reported in ppm referenced to the appropriate residual solvent peaks and coupling constants are reported in Hz. The multiplicity of signals is indicated using the following abbreviations: s = singlet, d = doublet, t = triplet, q = quadruplet, bs = broad singlet, bd = broad doublet, m = multiplet. Raman spectra were recorded with a Jobin and Yvon Lambram HR800 equipped with a helium neon laser (excitation line at 532 nm). DRX analyses were run by the Technical platform of the ICT (“Institut de Chimie de Toulouse”, FR2599). X-Ray diffraction patterns were collected at room temperature on a PANalytical X’Pert MPD Pro (θ - θ) diffractometer using Cu $K\alpha_1, K\alpha_2$ radiation. X-ray fluorescence measurements were performed in Energy Dispersive mode using the silicon drift detector installed on the WAXS diffractometer at CEMES (Amptek X-123 Super SDD, energy resolution 125 eV FWHM @ 5.9 keV). The source was a sealed tube with Mo anode operated at 50kV, so both Br and Pd K alpha lines could be effectively accessed (11.7-11.9 keV and 20.7-21.2 keV respectively). TEM analyses were run at the “Centre de MicroCaractérisation Raimond Castaing”. TEM micrographs of nanoparticles were obtained both dispersed in glycerol from a JEOL JEM 1400 microscope at 120 kV. The size distribution and average diameter were determined from TEM images based on Image-J software and a Microsoft Excel macro developed by Christian Pradel permitting to determine the mean size of spherical nanoparticles with the corresponding standard deviation for an important number of nanoparticles (thousands of them). EPR spectra were recorded on a Bruker Elexsys E500 spectrometer (Oxford).

GC-MS analyses were performed on a GC Perkin Elmer Clarus 500 with a flame ionization detector (FID) using a SGE BPX5 column (30 m x 0.32 mm x 0.25 mm) composed of 5% phenylmethylsiloxane and a Perkin Elmer Clarus 560 S mass spectrometer. The injector temperature was 250 °C and the flow was 2 mL/min. The temperature programme was 45 °C for 2 min, 20 °C/min to 300 °C, hold for 5 min.

Materials. Glycerol was dried under vacuum at 80 °C overnight prior to use. All reagents and other chemicals were purchased at the highest commercial quality and used without further purification unless noted otherwise. Solvents used for organic compounds extractions after catalysis: EtOAc, PhMe and/or CHCl₃. All reactions were performed under Ar atmosphere using standard Schlenk techniques and vacuum-line manipulations. The synthesis of the Pd Nanoparticles were performed in a Fischer-Porter bottle and the catalytic reactions in Schlenk tubes.

General Experimental Procedures.

Synthesis of PdNPs in glycerol. 0.10 mmol of palladium precursor (36 mg for PdI₂; 27 mg for PdBr₂; 18 mg for PdCl₂; 9.1 mg for Pd(OAc)₂; and PVP (Mn = 10000; 222 mg; Pd/monomer = 1/20) were dissolved in degassed glycerol (10 mL) and mixed under vacuum at r.t. in a Fischer-Porter bottle for 2 min. The system was then pressurized under 3 bar of H₂ and stirred at 80 °C overnight, resulted in a black colloidal suspension. Palladium NPs in the solid state (black powder) were isolated from glycerol solutions by centrifugation at 4000 rpm for 3 x 10 min and then decantation by adding acetone and ethanol.

General experimental procedure for the homocoupling of bromoarenes. An oven-dried Schlenk tube was charged with the starting material (1.0 mmol, 1 equiv.), KOH (1.0 mmol, 1 equiv.), and hydroquinone (0.5 mmol, 1 equiv.) under Ar. The catalytic solution in glycerol was then transferred to the reaction vessel under Ar. The reaction mixture was heated to 90 °C and it

was vigorously stirred with a PTFE coated Niobium magnetic stirrer for 18 h. The catalytic solution was then extracted with EtOAc (PhMe or CHCl_3) and the combined organic extracts were then evaporated under reduced pressure. The reaction crudes were then analyzed by ^1H -NMR or GC-MS using dodecane or 1,1,2,2-tetrachloroethane as internal standards. The reaction crude was then purified by silica gel flash chromatography to furnish the desired homocoupling products (**4-13**).

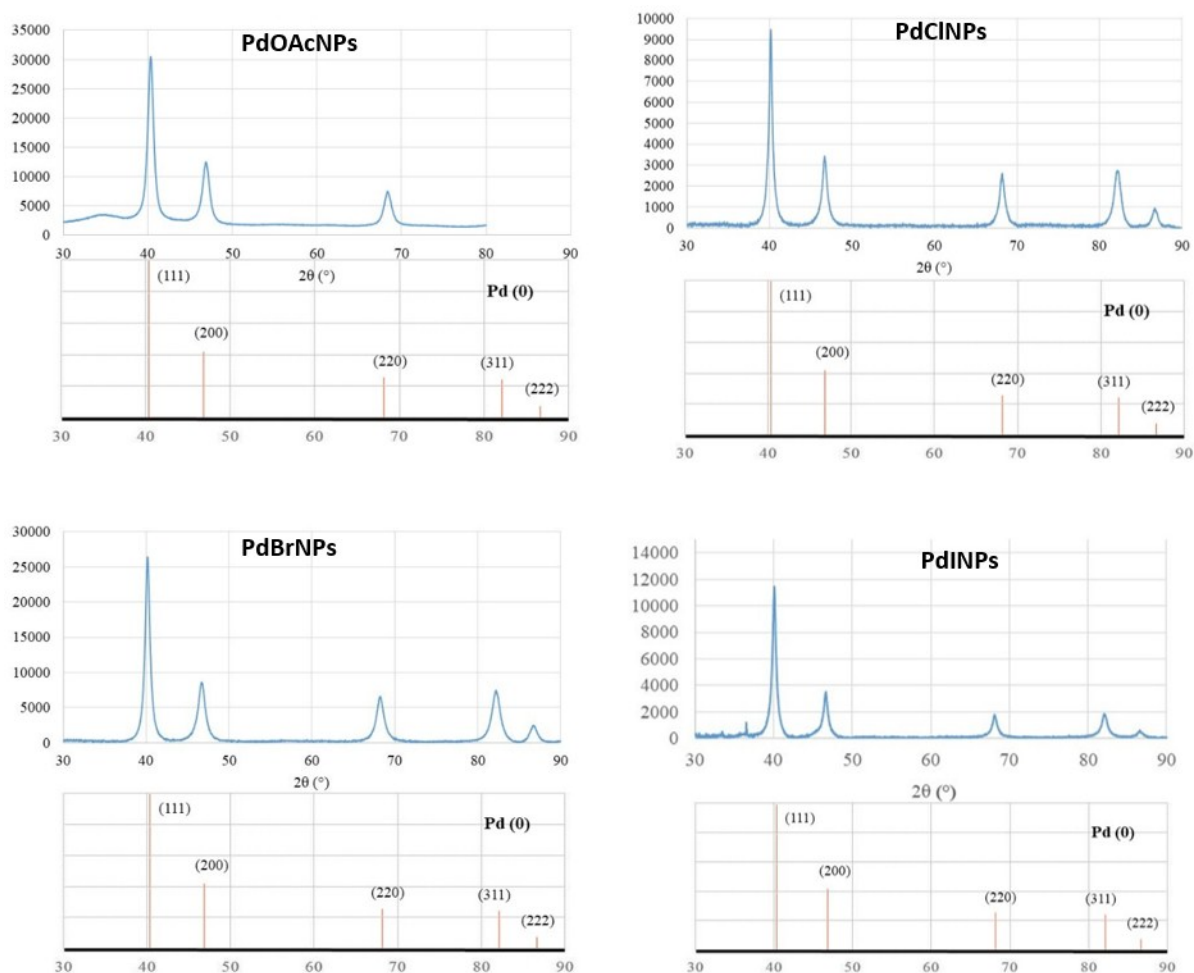
B. Characterization of preformed palladium nanoparticles, PdXNPs

Figure S1. Powder X-Ray Diffraction diffractograms of palladium nanoparticles stabilized by PVP: PdOAcNPs, PdCINPs, PdBrNPs, and PdINPs. For each of them, the XRD pattern corresponding to the fcc Pd(0) structure is added with the assignment of the corresponding crystallographic planes (COD code: 00-005-0681).

Electronic Supplementary Information

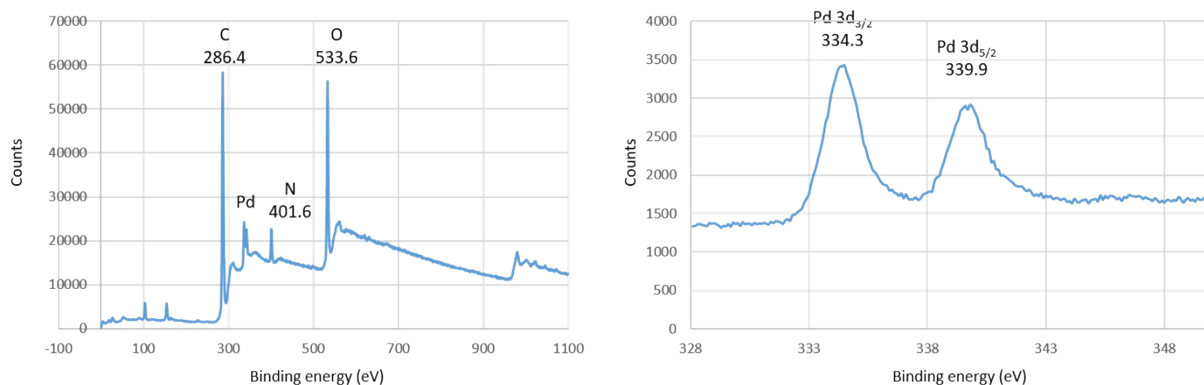


Figure S2. XPS survey spectrum for PdOAcNPs (left) and the corresponding high-resolution spectrum in the Pd 3d binding energy region (right). Note: the binding energies for PdO appear at *ca.* 337 and 342 eV.

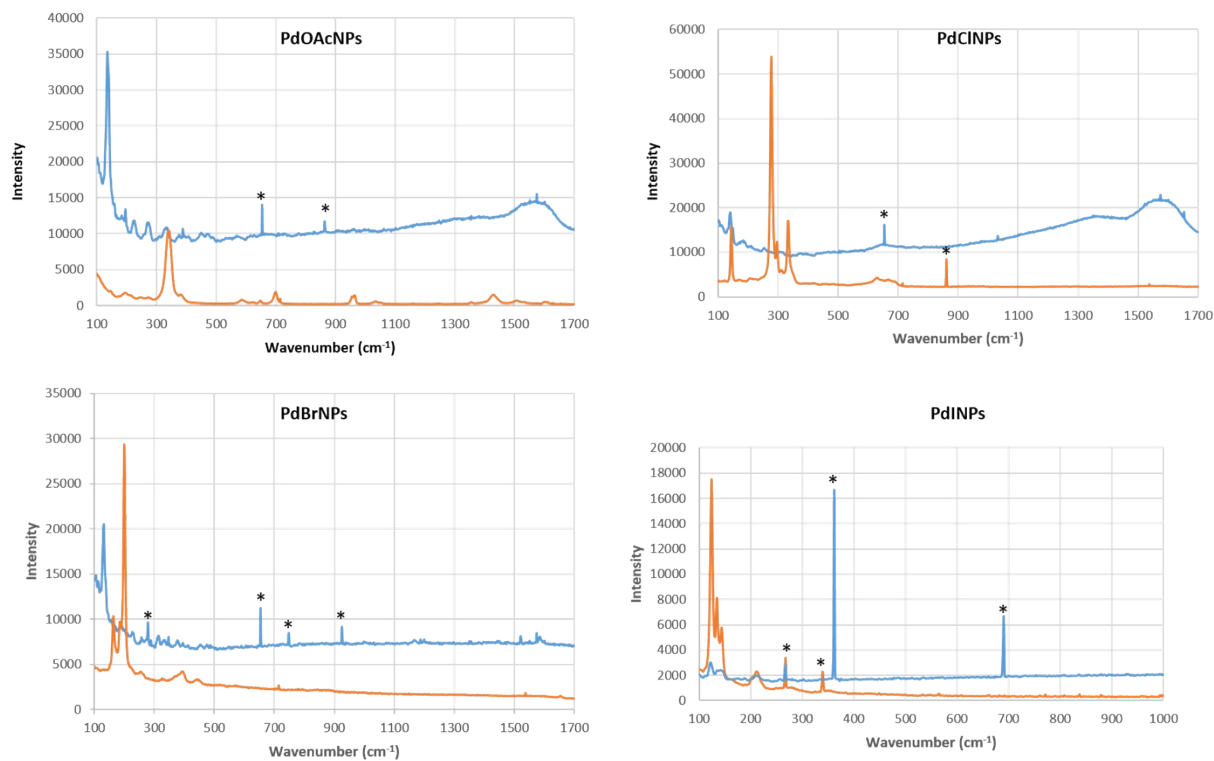
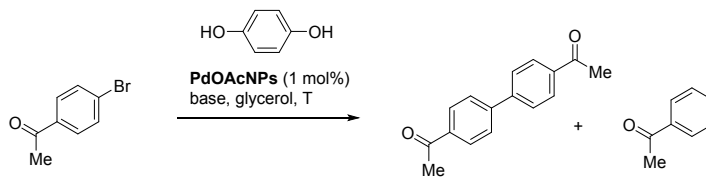


Figure S3. Raman spectra for PdOAcNPs, PdClNPs, PdBrNPs, and PdINPs (blue traces) and their corresponding palladium precursors ($\text{Pd}(\text{OAc})_2$, PdCl_2 , PdBr_2 , and PdI_2 ; orange traces). * denotes artifact signal.

C. Reaction Optimization Studies

Table S1. Reaction optimization conditions for the homo-coupling reaction of 4'-bromoacetophenone with preformed PdNPs prepared from Pd(OAc)₂, named PdOAcNPs.

Entry	HQ	Base	T (°C)	Conv. (%) ^a	Yield (%) ^a	Selectivity ratio (bis-aryl:acetophenone) ^a
1	1 equiv.	---	90	44 ^b	39	9:1
2	1 equiv.	NaOH 1 equiv.	90	68 ^b	17 ^b	11:1 ^b
3	1 equiv.	KOH 1 equiv.	90	68	61	9:1
4	1 equiv.	Na ₂ CO ₃ 1 equiv.	90	60 ^b	23 ^b	9:1 ^b
5	1 equiv.	Et ₃ N 1 equiv.	90	65	52	7:1
6	---	KOH 1 equiv.	90	24	6	3:7
7	0.5 equiv.	KOH 1 equiv.	90	57	55	18:1
8	2 equiv.	KOH 1 equiv.	90	66	59	9:1
9	6 equiv.	KOH 1 equiv.	90	4 ^b	n.d.	1:1 ^b
10	1 equiv.	KOH 1 equiv.	120	86	75	7:1
11 ^e	1 equiv.	KOH 1 equiv.	90	37	6	2.25:1

All reactions were carried out at 1 mmol scale of substrate and 1 mol % of catalyst (1 mL of preformed catalytic solution), and heated to 90 °C for 18 h (unless otherwise stated). After 18 h the catalytic phase was analyzed by GC-MS (EI+) with EtOH. After extraction with CH₂Cl₂ (7x3 mL) the « crude » product was analyzed by both GC-MS (EI+) and ¹H NMR with an internal standard (internal standard (IS), 1 mmol > n(IS) > 0.1 mmol). Not determined (n.d.); ^a Determined by ¹H RMN; ^b Determined by GC-MS (with dodecane as standard); ^c Reaction carried out at 2 mmol of substrate; ^d 60 h reaction time; ^e Results when the catalytic phase was reused in a 2nd run, from that used in the catalytic reaction of entry 7 in Table 1 of the main text.

D. TEM analysis after catalysis

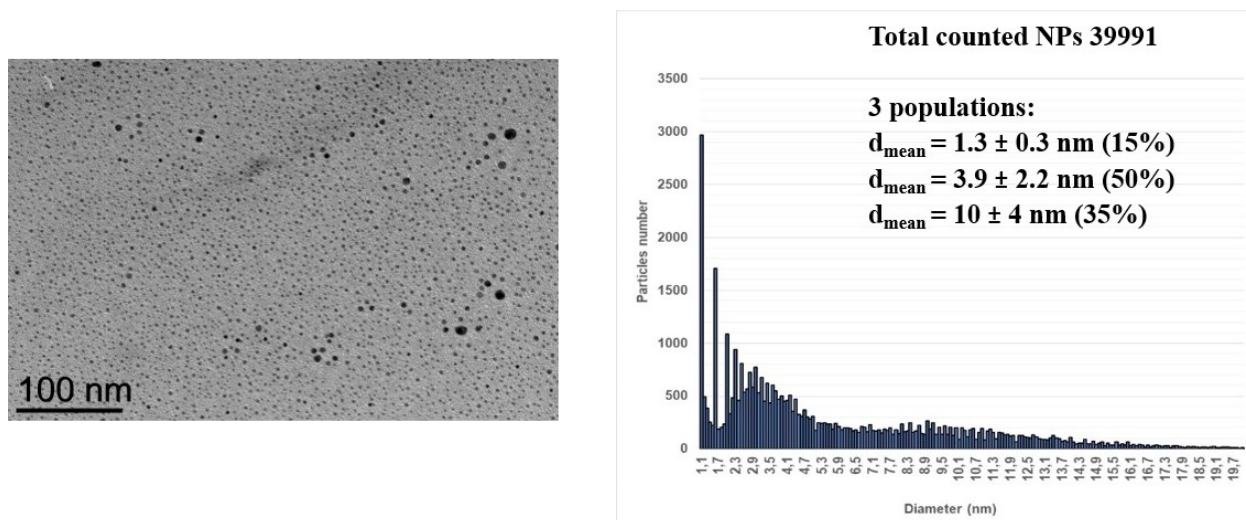


Figure S4. TEM analysis of PdOAcNPs after being used in catalysis (from the experiment described in entry 7 of Table 1 of the main text)

E. TEM analysis of Pd/C dispersed in glycerol

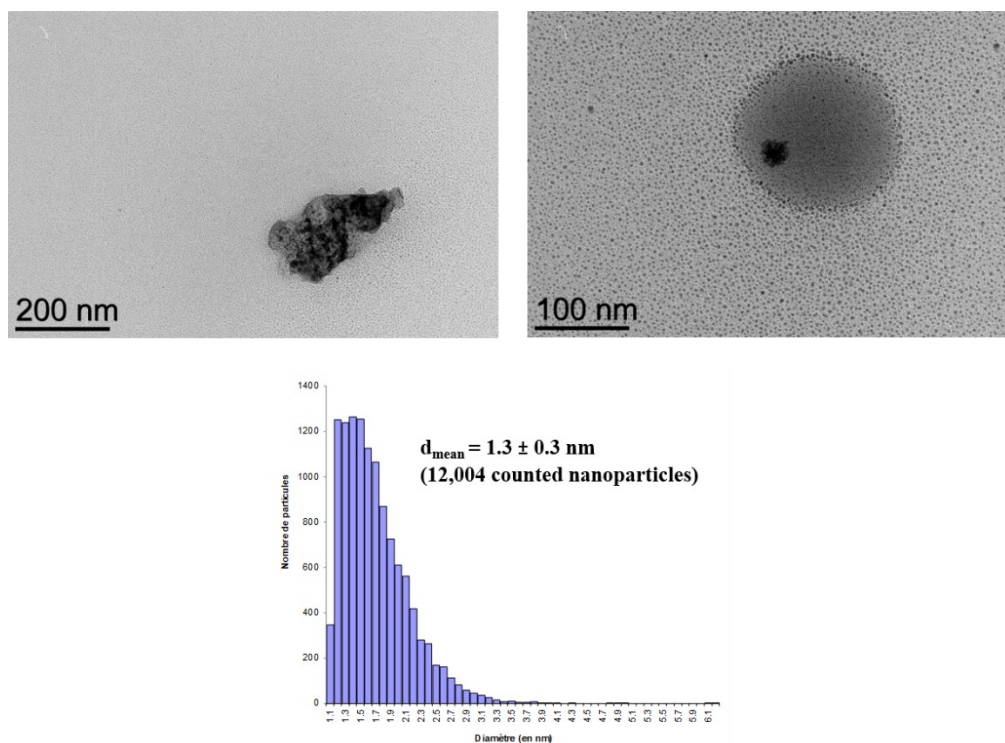
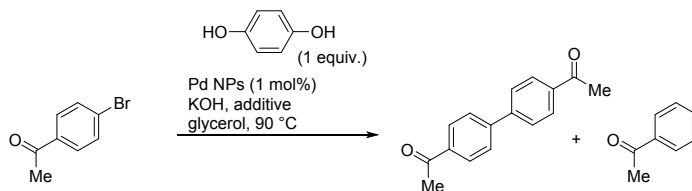
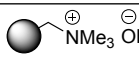
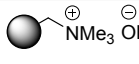


Figure S5. TEM analysis of commercial Pd/C (10 wt % metal loading on matrix activated carbon support) dispersed in glycerol.

F. Halide effect studies

Table S2. Halide effect study on the homo-coupling reaction using preformed PdNPs as catalysts in glycerol.

Entry	KOH	PdNPs	Additive	Conv. (%)	Selectivity (bis-aryl:acetophenone)	Yield (bis-aryl)
1	1 equiv.	PdOAcNPs	KI 0.20 equiv.	9%	5.6:4.4	5%
2	0.2 equiv.	PdOAcNPs	 1 equiv.	67%	9.4:0.6	63%
3	---	PdOAcNPs	 1 equiv.	33%	9.1:0.9	30%
4	1 equiv.	PdOAcNPs	NaOAc 2 equiv.	64%	9.4:0.6	60%
5	1 equiv.	PdINPs	NaOAc 2 equiv.	8%	2.5:7.5	2%

All reactions were carried out at 1 mmol scale of substrate and 1 mol % of catalyst (1 mL of preformed catalytic solution), and heated to 90 °C for 18 h (unless otherwise stated). After 18 h the catalytic phase was analyzed by GC-MS (EI+) with EtOH. After extraction with CH₂Cl₂ (7x3 mL) the « crude » product was analyzed by both GC-MS (EI+) and ¹H NMR with an internal standard (internal standard (IS), 1 mmol > n(IS) > 0.1 mmol). Not determined (n.d.); ^a 72 h.

G. Determination of bromine content by X-ray fluorescence measurements

PdBrNPs, before and after catalysis, were sealed in low absorption glass capillaries of 1.5 mm in diameter. Since the instrument only provides raw fluorescence data, another sample of PdBr_2 was also prepared as a reference. In order to get low and similar global absorption (so-called matrix effect), pure PdBr_2 was carefully dispersed in a large amount of PVP. For all samples, measurement time was 2 h.

Using the calibration from PdBr_2 , the molar ratio Br/Pd could be estimated to 0.0274 before catalysis, and 0.0567 after catalysis. Uncertainty is difficult to estimate and may be as high as 10%, but these results clearly indicate a strong increase of the Br/Pd ratio after catalysis due to the release of bromine from the substrate (4-bromoacetophenone).

H. Mechanistic insights for the homo-coupling reaction.

A comparative analysis between the experimental EPR spectrum and a simulation of the the corresponding spectra of anion radical species of 4'-bromoacetophenone (**I**), hydroquinone (**II**) and acetophenone (**III**) do not match with the presence of acetophenone radicals in the reaction mixture.

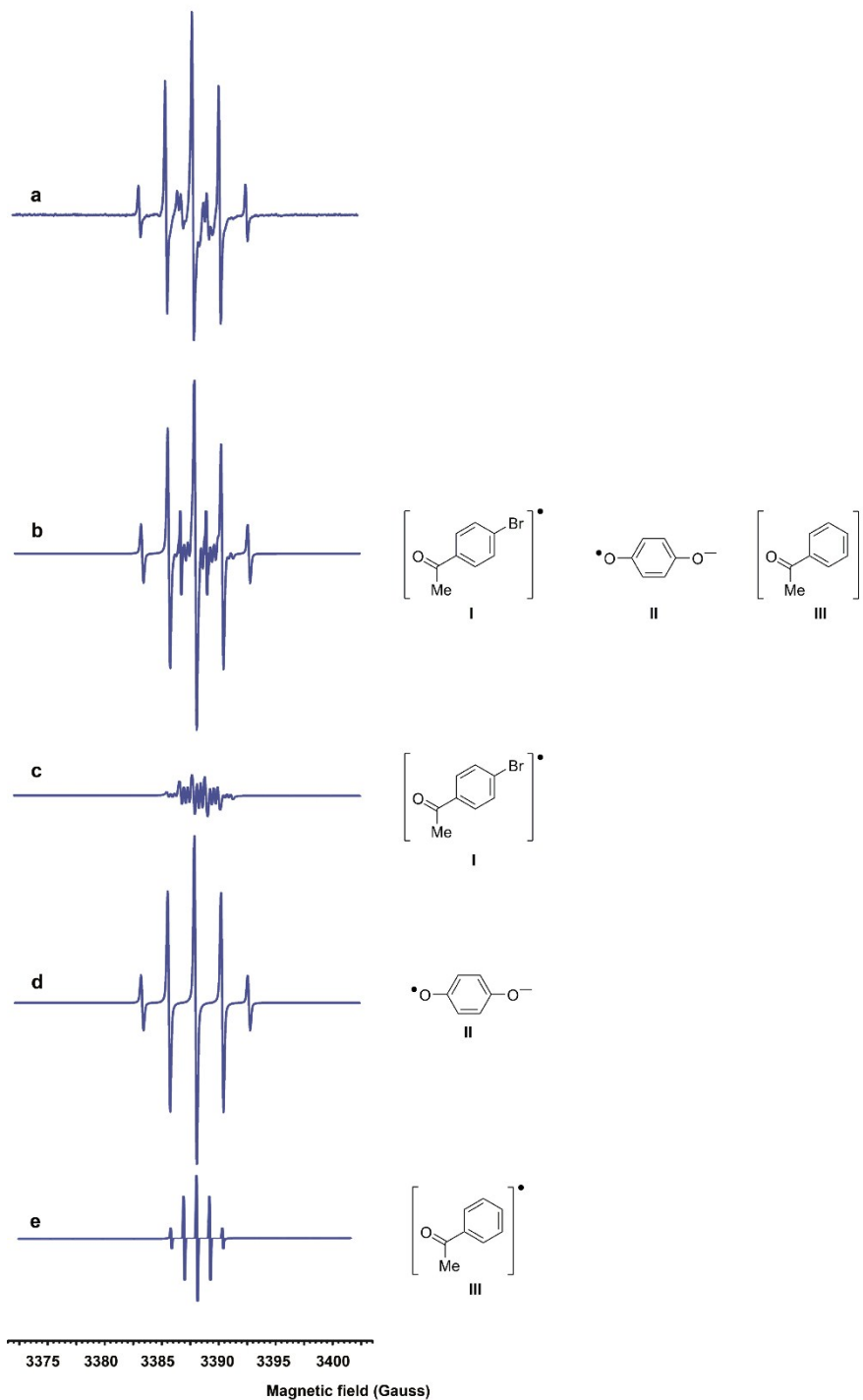


Figure S6. EPR spectra: a) Experimental EPR spectrum of the reaction sample; b) Superposition of simulated EPR spectra of the anion radical species of 4'-bromoacetophenone (**I**), hydroquinone (**II**) and acetophenone radical (**III**); c) Simulated EPR spectrum of 4'-bromoacetophenone anion radical (species **I**); d) Simulated EPR spectrum of hydroquinone anion radical (species **II**); e) Simulated EPR spectrum of acetophenone radical (species **III**).

Further experiments to elucidate the role of the base on the reaction mechanism were carried out. In particular we sought if the hypothesized highly reactive aryl-radical species ($\text{Ar}\cdot$) arising from fragmentation of aryl radical anion $[\text{Ar-X}]^{\bullet-}$ could react with an arene to give a cyclohexadienyl radical, which would be then deprotonated with KOH to generate a biaryl radical anion. This radical anion could then transfer an electron to another molecule of aryl bromide reactant to yield the desired product along with an arene radical anion $[\text{Ar-X}]^{\bullet-}$, thereby closing the catalytic cycle.¹ However, our tests employing up to 10 equiv. excess of different arenes [namely, fluorobenzene, α,α,α -trifluorotoluene and 1,3-bis(trifluoromethyl)benzene] were unsuccessful to provide any cross-coupling product.

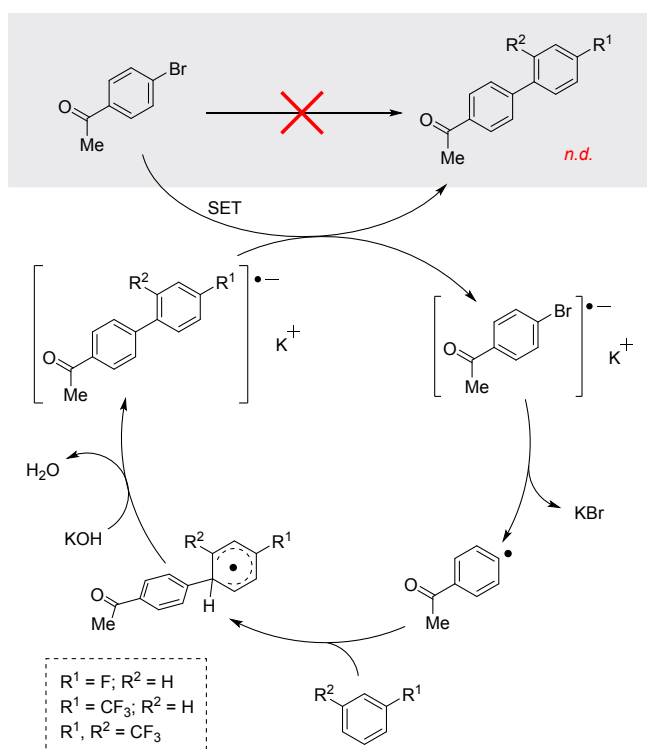
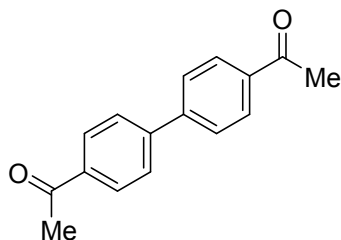


Figure S7. A base-promoted homolytic aromatic substitution mechanism has been refuted.

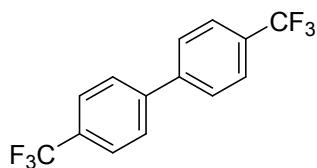
n.d. denotes not detected.

I. Characterization of bis-aryls 4, 6-8, 10, 11, 13.



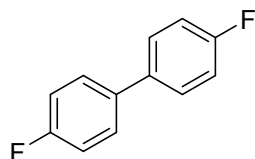
4,4'-Bisacetylbiphenyl (4). Following the general procedure for the homo-coupling reaction and starting from **1** (995.2 mg, 5.0 mmol), the product was obtained as a white solid (404.0 mg, 68%) by silica gel chromatography and elution with pentane/EtOAc (100:0 and 80:20). Characterization data matches literature reports.^{2, 3}

¹H NMR (300 MHz, CDCl₃) δ 8.06 (d, *J* = 8.7 Hz, 4H), 7.72 (d, *J* = 8.7 Hz, 4H), 2.65 (s, 6H). ¹³C NMR (75 MHz, CDCl₃) δ 197.7, 144.5, 136.7, 129.1, 127.6, 26.9. MS (EI) 238 (M), 239 (M+1).



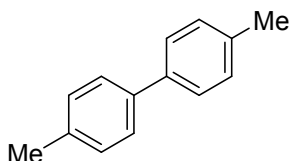
4,4'-Trifluoromethylbiphenyl (6). Following the general procedure for the homo-coupling reaction and starting from 4-bromo-1-trifluoromethylbenzene (140 μL, 1.0 mmol), the product was obtained as a white solid (94.1 mg, 65%) by silica gel chromatography and elution with pentane/EtOAc (100:0 and 95:5). Characterization data matches literature reports.⁴

¹H NMR (300 MHz, CDCl₃) δ 7.80-7.69 (m, 8H). ¹³C NMR (75 MHz, CDCl₃) δ 143.4, 130.4 (d, *J* = 32.5 Hz), 127.8, 126.1 (q, *J* = 3.8 Hz), 124.3 (d, *J* = 272.1 Hz). ¹⁹F NMR (282 MHz, CDCl₃) δ -62.6. MS (EI) 290 (M), 291 (M+1).



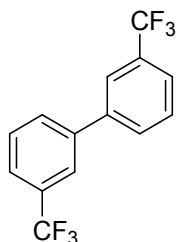
4,4'-difluorobiphenyl (7). Following the general procedure for the homo-coupling reaction and starting from 1-bromo-4-fluorobenzene (110 μL , 1.0 mmol), the product was obtained as a white solid (63.7 mg, 67%) by silica gel chromatography and elution with pentane/EtOAc (100:0 and 90:10). Characterization data matches literature reports.^{5, 6}

^1H NMR (300 MHz, CDCl_3) δ 7.55 – 7.45 (m, 4H), 7.18 – 7.07 (m, 4H). ^{13}C NMR (75 MHz, CDCl_3) δ 162.6 (d, $J = 246.4$ Hz), 136.5 (d, $J = 3.4$ Hz), 128.7 (d, $J = 8.0$ Hz), 115.8 (d, $J = 21.5$ Hz). ^{19}F NMR (282 MHz, CDCl_3) δ -115.8 (ddd, $J = 14.0, 8.8, 5.3$ Hz). MS (EI) 190 (M), 191 (M+1).



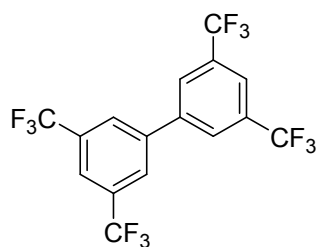
4,4'-Dimethylbiphenyl (8). Following the general procedure for the homo-coupling reaction and starting from 4-bromotoluene (123 μL , 1.0 mmol), the product was obtained as a white solid (10.9 mg, 12%) by silica gel chromatography and elution with pentane/EtOAc (100:0 and 95:5). Characterization data matches literature reports.^{2, 7, 8}

^1H NMR (300 MHz, CDCl_3) δ 7.52 (d, $J = 8.2$ Hz, 4H), 7.27 (d, $J = 7.6$ Hz, 1H), 2.43 (s, 6H). ^{13}C NMR (75 MHz, CDCl_3) δ 138.4, 136.8, 129.6, 126.9, 21.2. MS (EI) 182 (M), 183 (M+1).



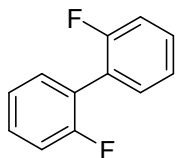
3,3'-Bis(trifluoromethyl)biphenyl (10). Following the general procedure for the homo-coupling reaction and starting from 3-bromo-1-trifluoromethylbenzene (140 μ L, 1.0 mmol), the product was obtained as a yellowish oil (124.7 mg, 86%) by silica gel chromatography and elution with pentane/EtOAc (100:0 and 90:10). Characterization data matches literature reports.^{9, 10}

¹H NMR (300 MHz, CDCl₃) δ 7.84 (bs, 2H), 7.80 – 7.75 (m, 2H), 7.71 – 7.64 (m, 2H), 7.62 (d, J = 7.6 Hz, 2H). ¹³C NMR (75 MHz, CDCl₃) δ 140.7, 131.6 (d, J = 32.5 Hz), 130.7 (d, J = 1.5 Hz), 129.7, 127.0 (s), 124.9 (q, J = 3.8 Hz), 124.2 (q, J = 3.8 Hz), 124.2 (d, J = 272.4 Hz). ¹⁹F NMR (282 MHz, CDCl₃) δ -62.6. MS (EI) 291 (M+1).



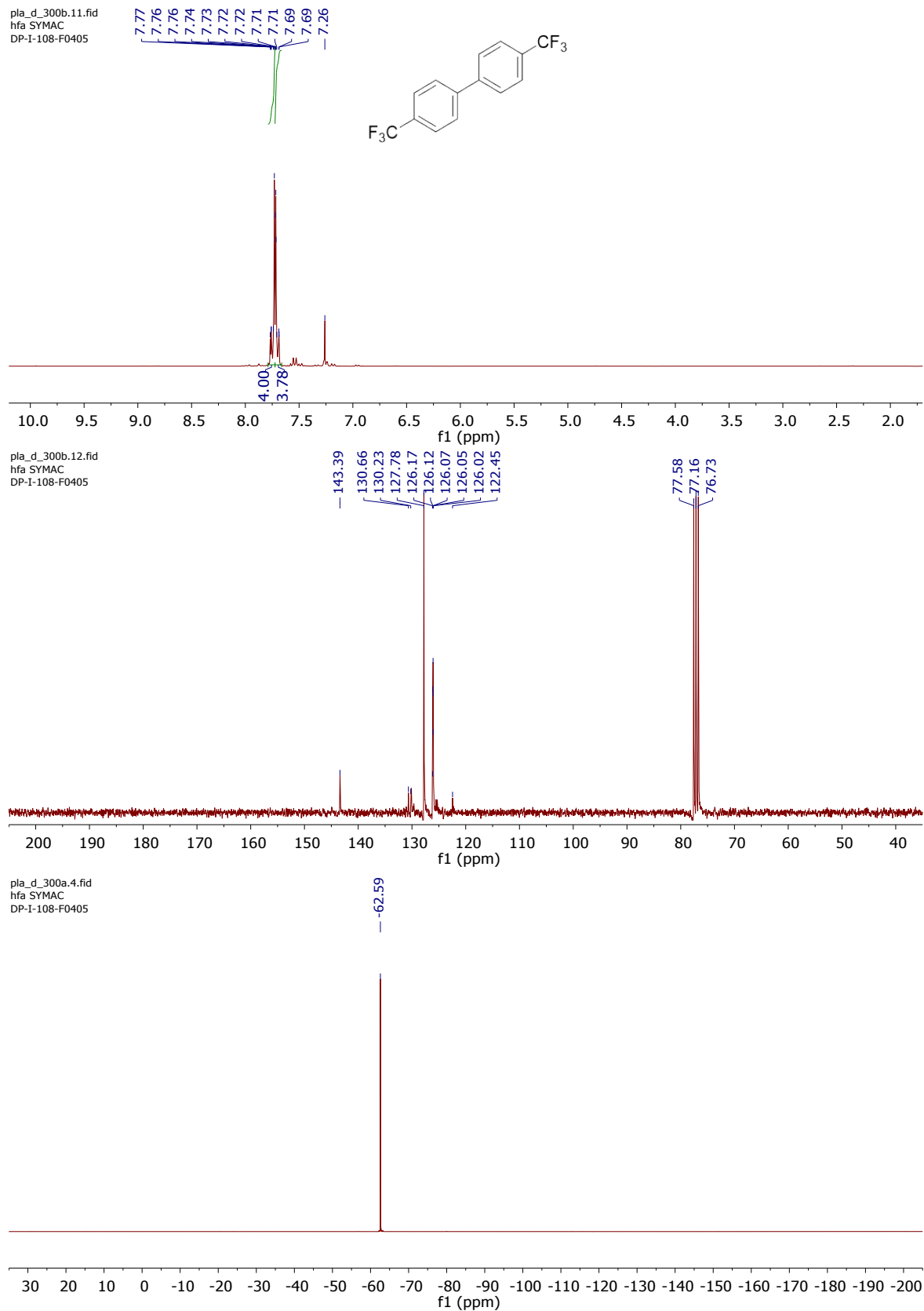
3,5,3',5'-Tetrakis(trifluoromethyl)biphenyl (11). Following the general procedure for the homo-coupling reaction and starting from 3,6-bis(trifluoromethyl)bromobenzene (173 μ L, 1.0 mmol), the product was obtained as a white solid (40.5 mg, 19%) by silica gel chromatography and elution with pentane. Characterization data matches literature reports.¹¹

^1H NMR (300 MHz, CDCl_3) δ 8.03 (bs, 4H), 7.99 (d, $J = 0.8$ Hz, 2H). ^{13}C NMR (75 MHz, CDCl_3) δ 140.6, 133.0 (q, $J = 33.8$ Hz), 127.7 (d, $J = 2.9$ Hz), 125.0 (t, $J = 272.6$ Hz), 122.8 (sep, $J = 4.1$ Hz). ^{19}F NMR (282 MHz, CDCl_3) δ -62.9. MS (EI) 427 (M+1).

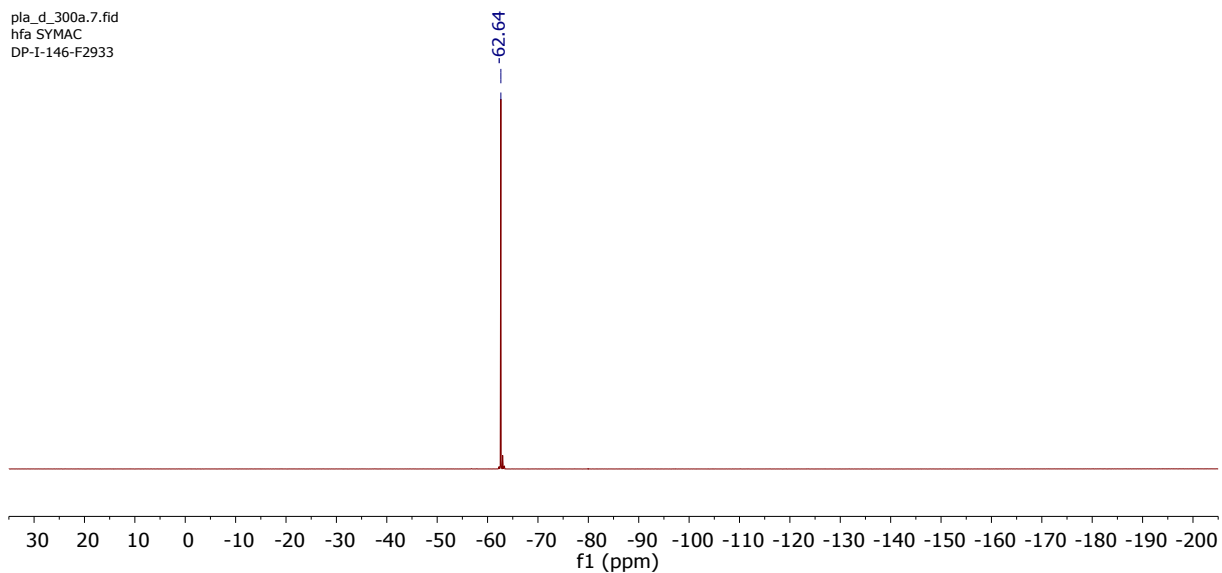
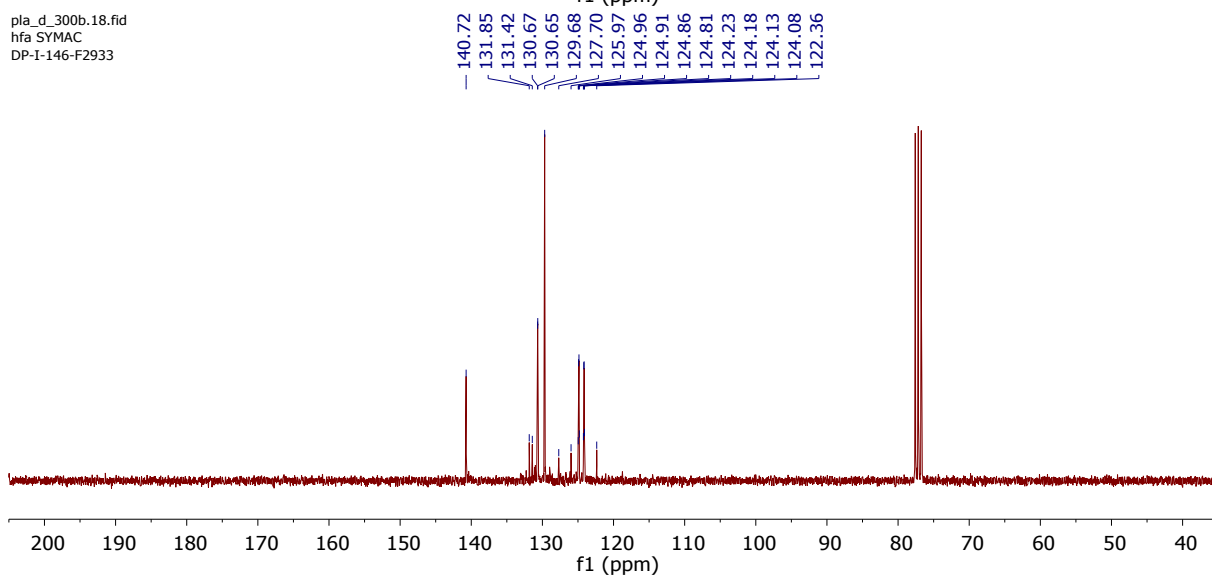
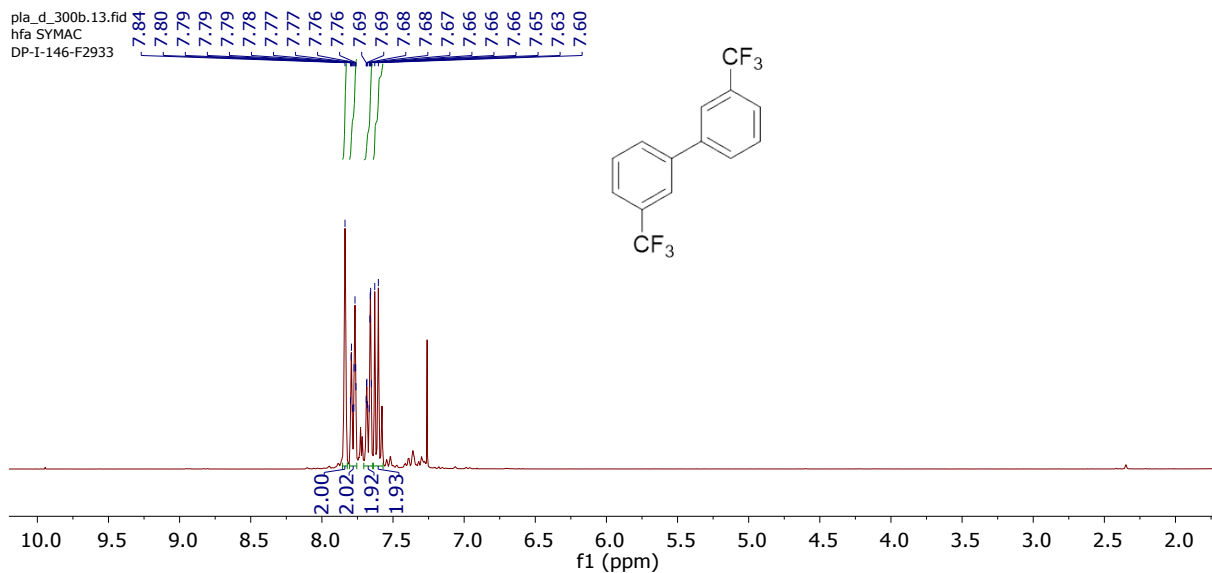


2,2'-Difluorobiphenyl (13). Following the general procedure for the homo-coupling reaction and starting from 1-bromo-2-fluorobenzene (109 μL , 1.0 mmol), the product was obtained as a white solid (67.5 mg, 71%) by silica gel chromatography and elution with pentane/EtOAc (100:0 and 90:10). Characterization data matches literature reports.^{12, 13}

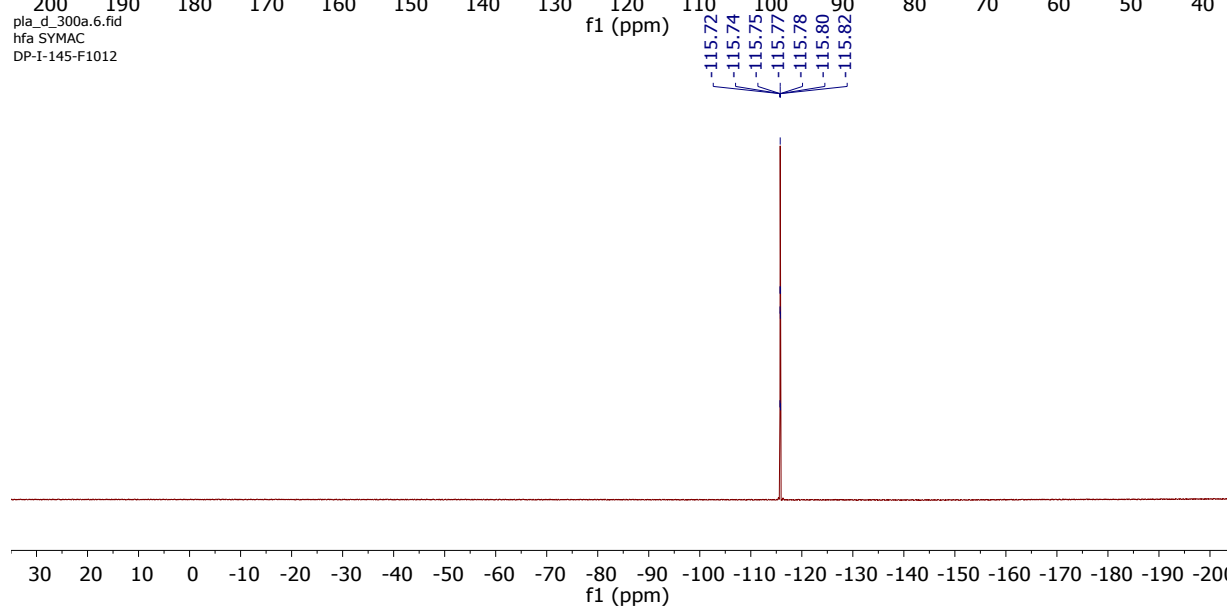
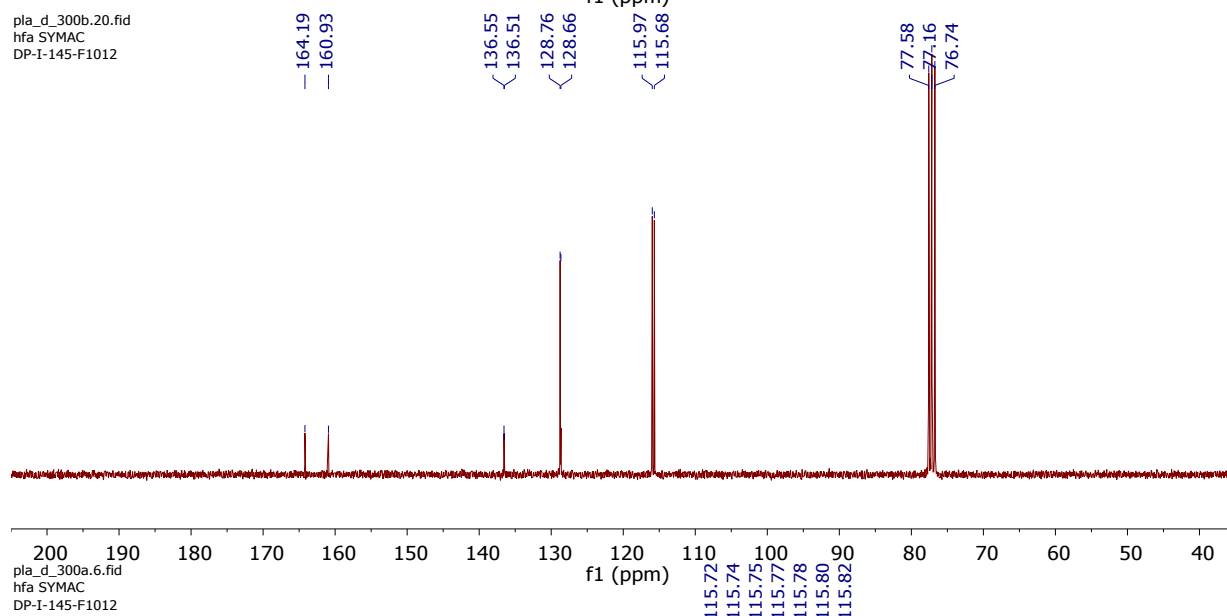
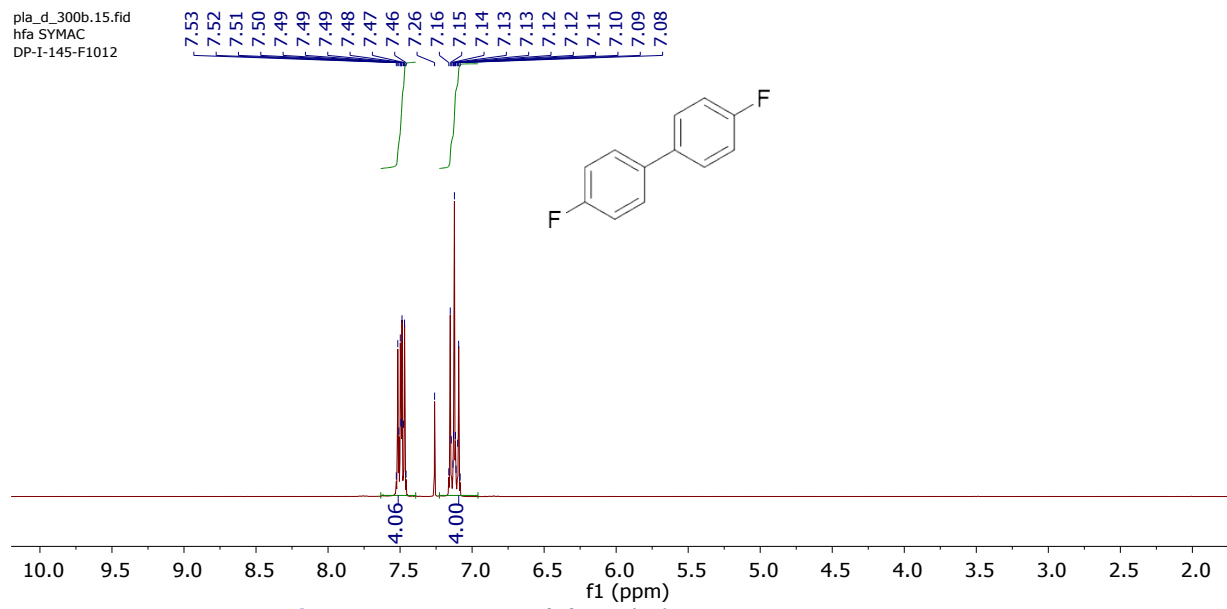
^1H NMR (300 MHz, CDCl_3) δ 7.47 – 7.36 (m, 4H), 7.31 – 7.17 (m, 4H). ^{13}C NMR (75 MHz, CDCl_3) δ 160.0 (dd, $J = 249.8, 1.7$ Hz), 131.7 (t, $J = 2.5$ Hz), 129.9 (t, $J = 4.2$ Hz), 124.2 (t, $J = 1.8$ Hz), 123.7 (dd, $J = 9.7, 5.5$ Hz), 117.34 – 115.12 (m). ^{19}F NMR (282 MHz, CDCl_3) δ -114.8 (d, $J = 6.0$ Hz). MS (EI) 190 (M), 191 (M+1).

J. ^1H , ^{13}C , and ^{19}F NMR Spectra of Selected Compounds 4, 6-8, 10, 11, 13.

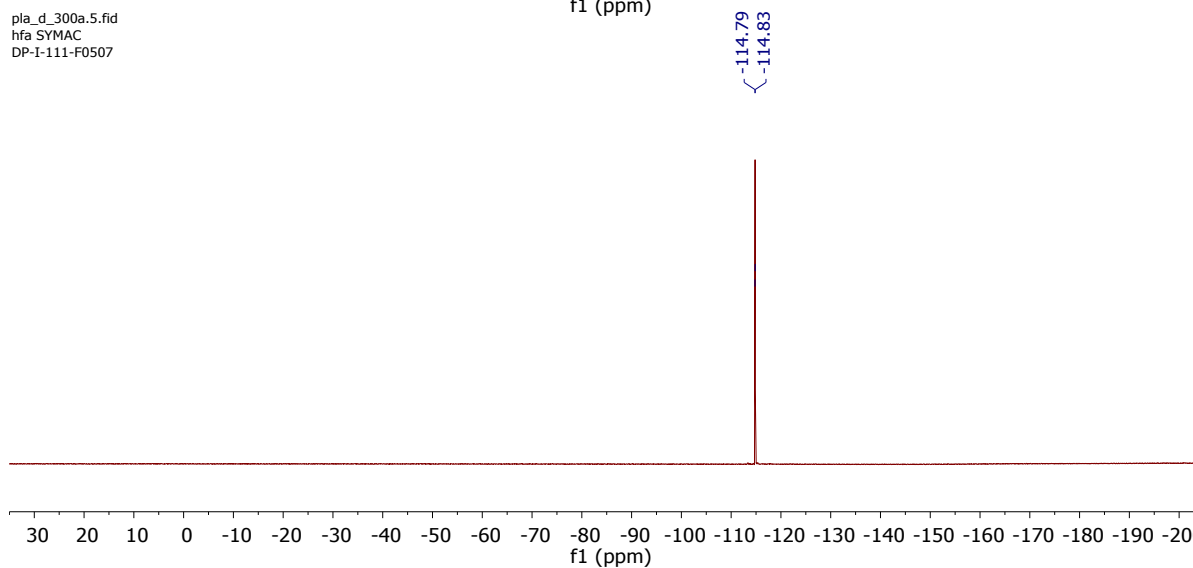
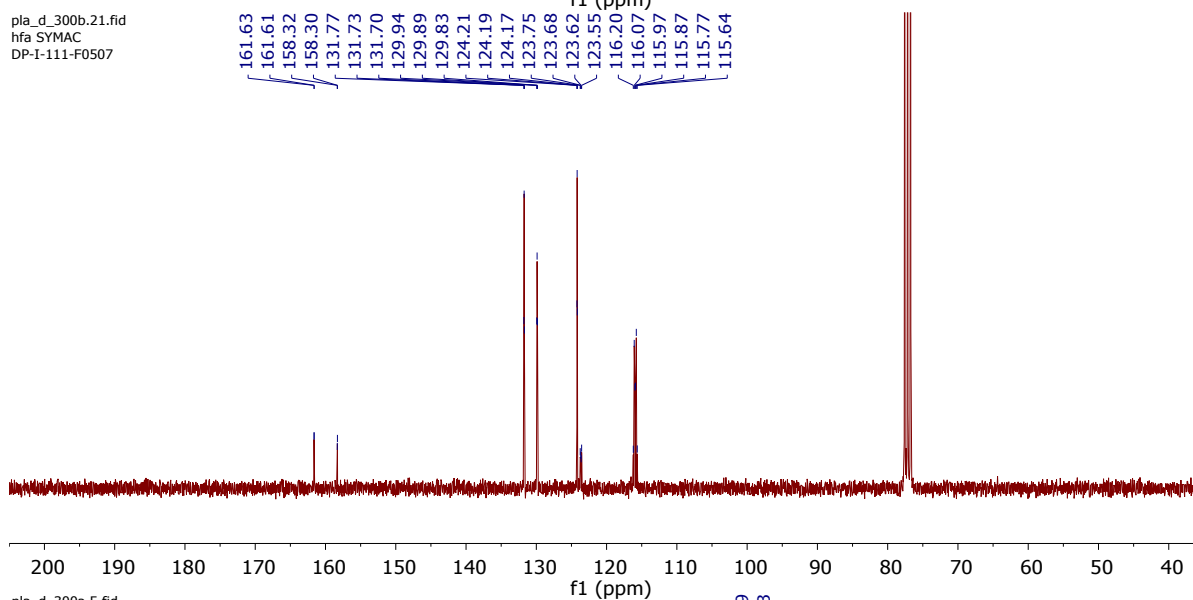
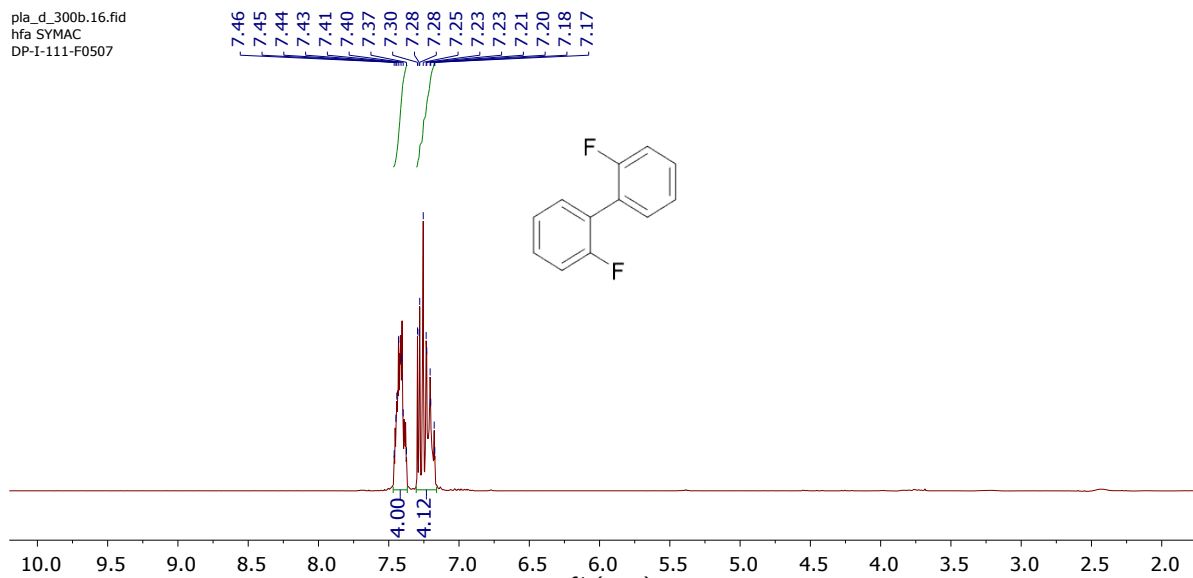
Electronic Supplementary Information



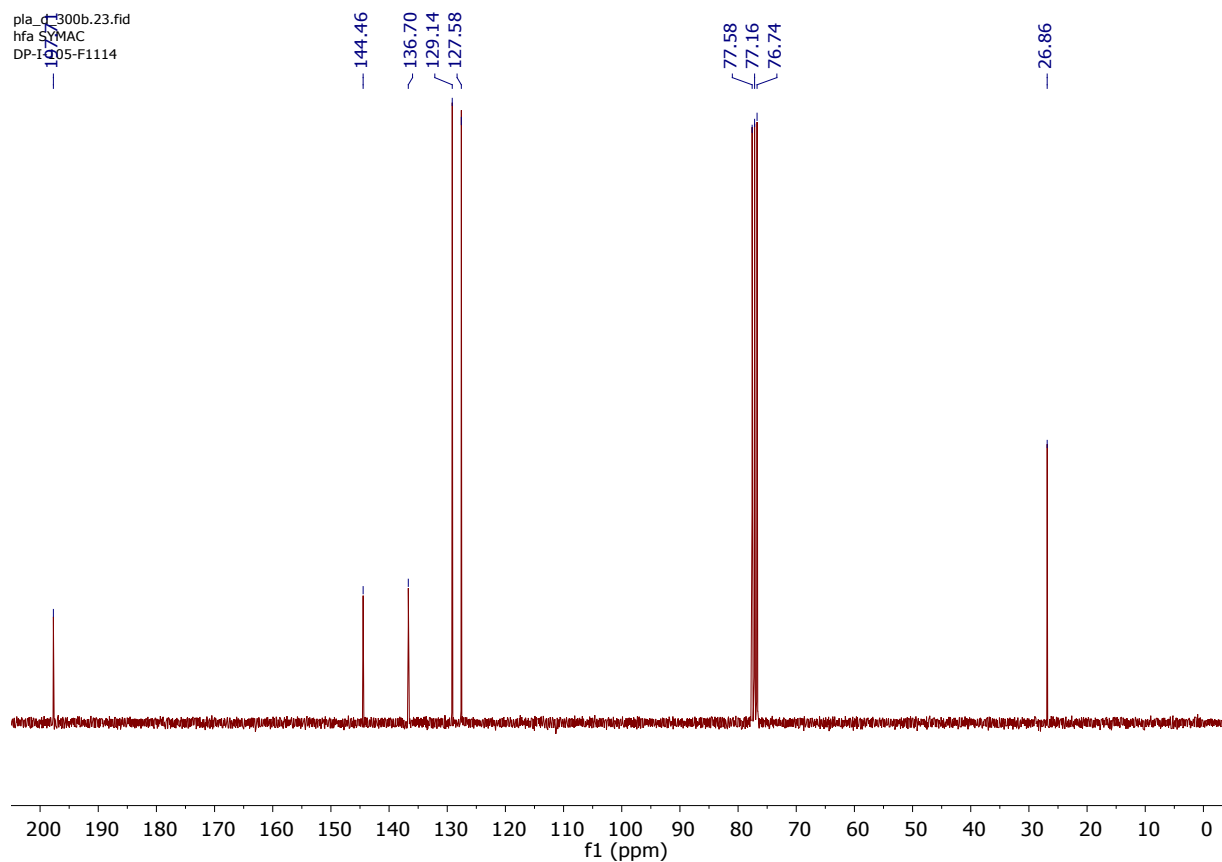
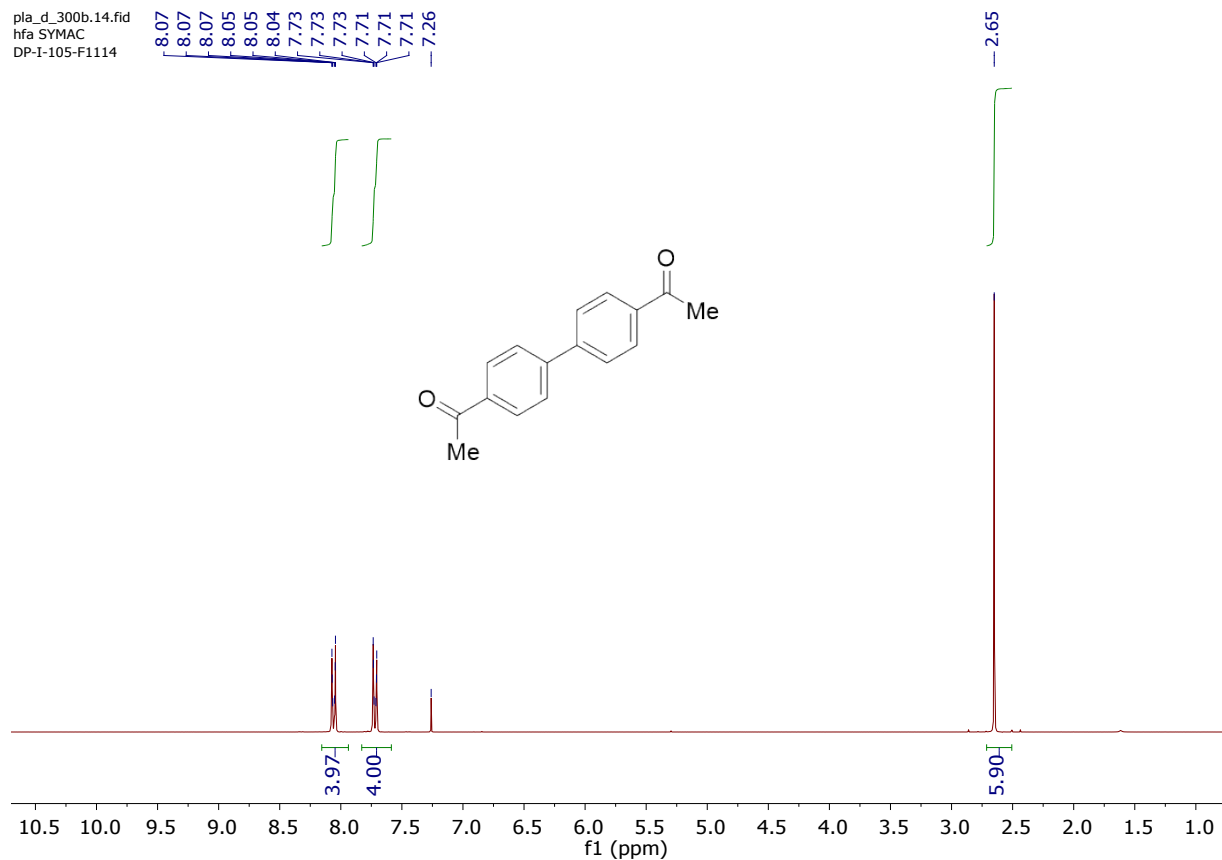
Electronic Supplementary Information



Electronic Supplementary Information

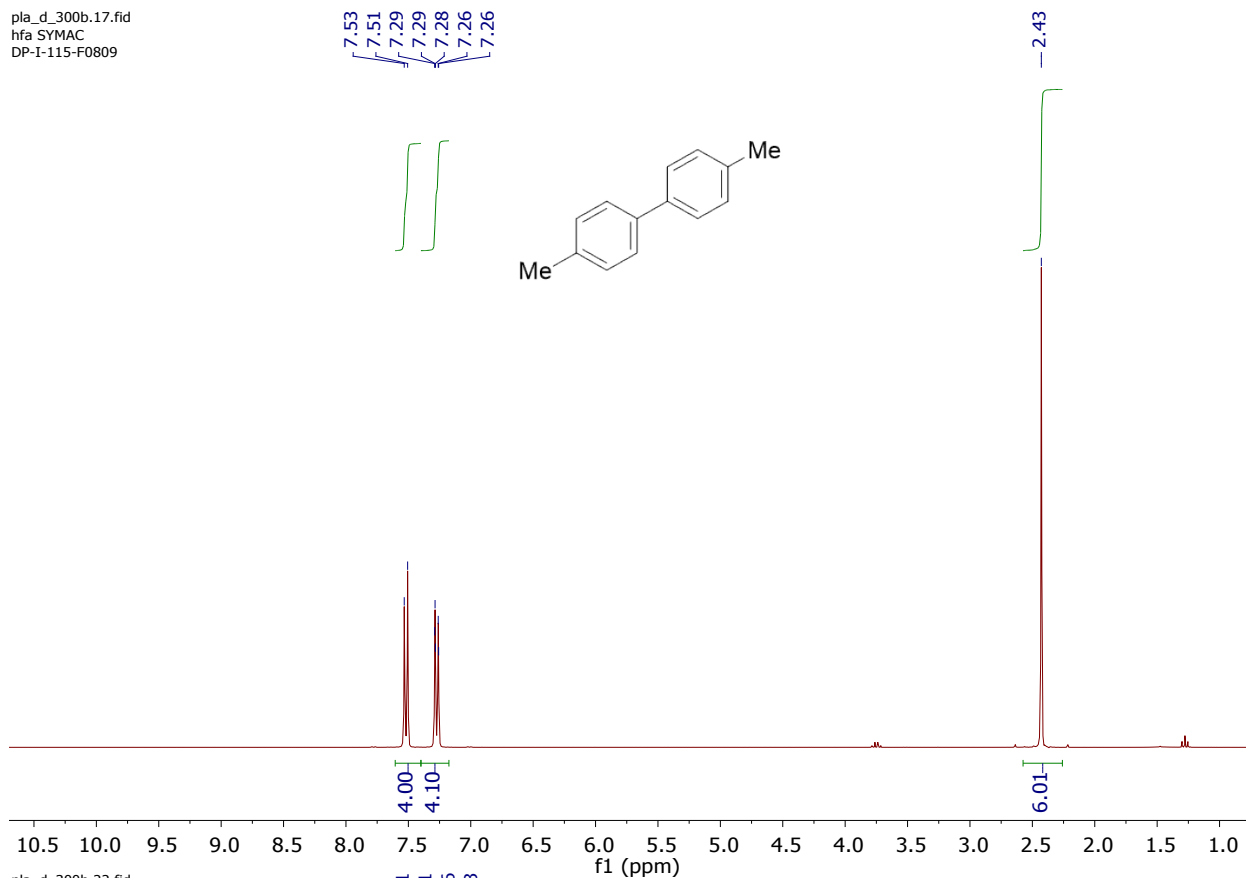


Electronic Supplementary Information

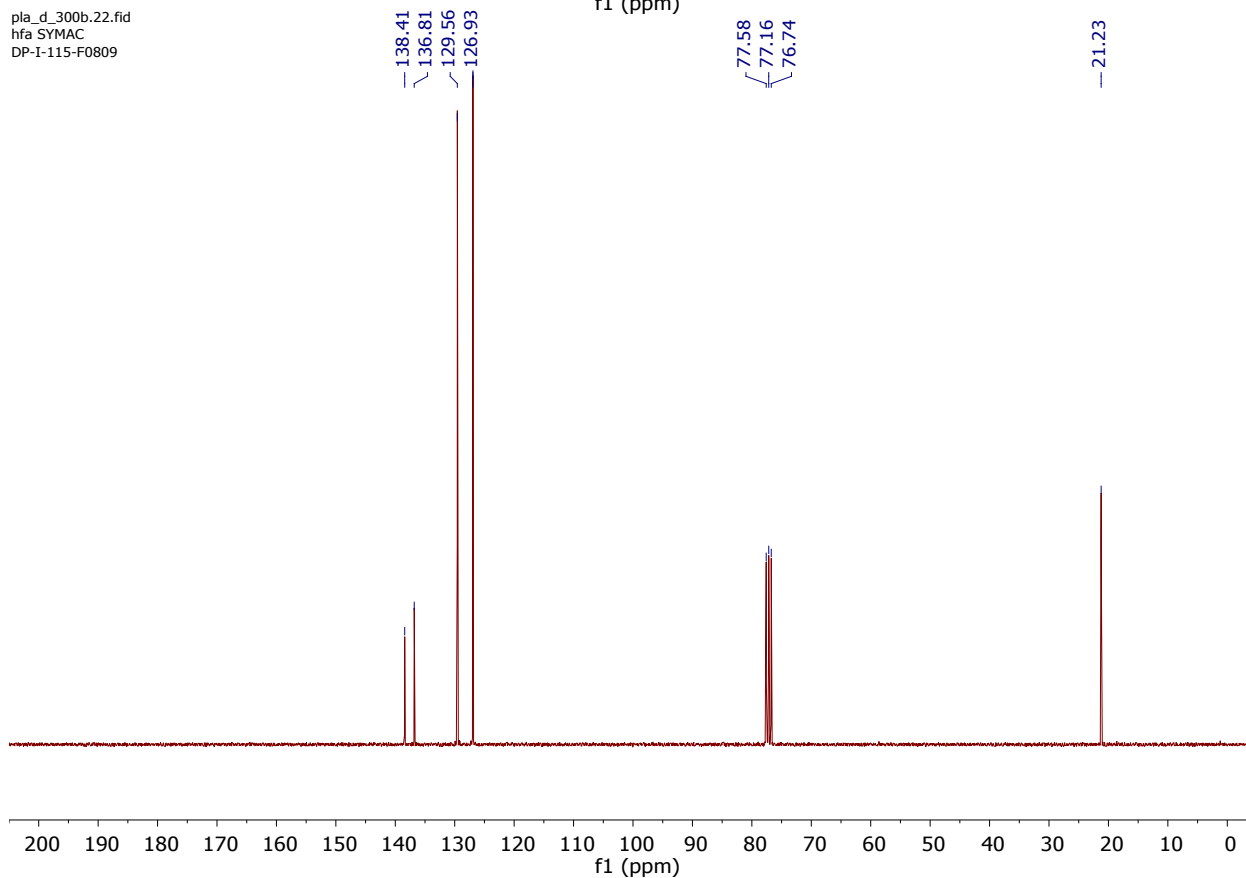


Electronic Supplementary Information

pla_d_300b.17.fid
hfa SYMAC
DP-I-115-F0809

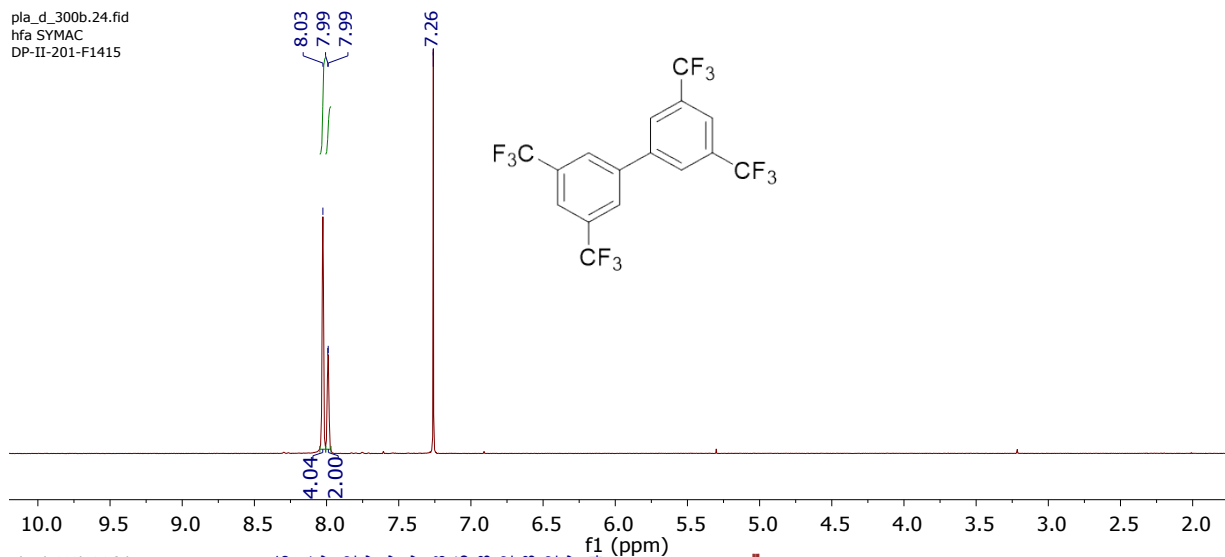


pla_d_300b.22.fid
hfa SYMAC
DP-I-115-F0809

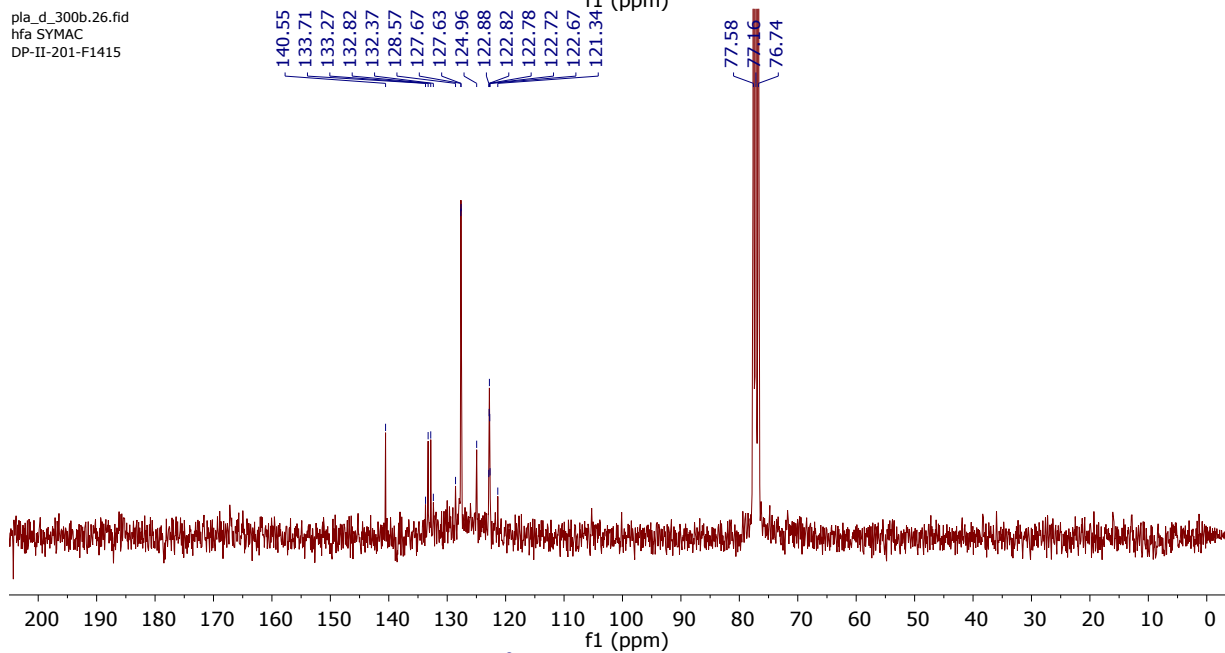


Electronic Supplementary Information

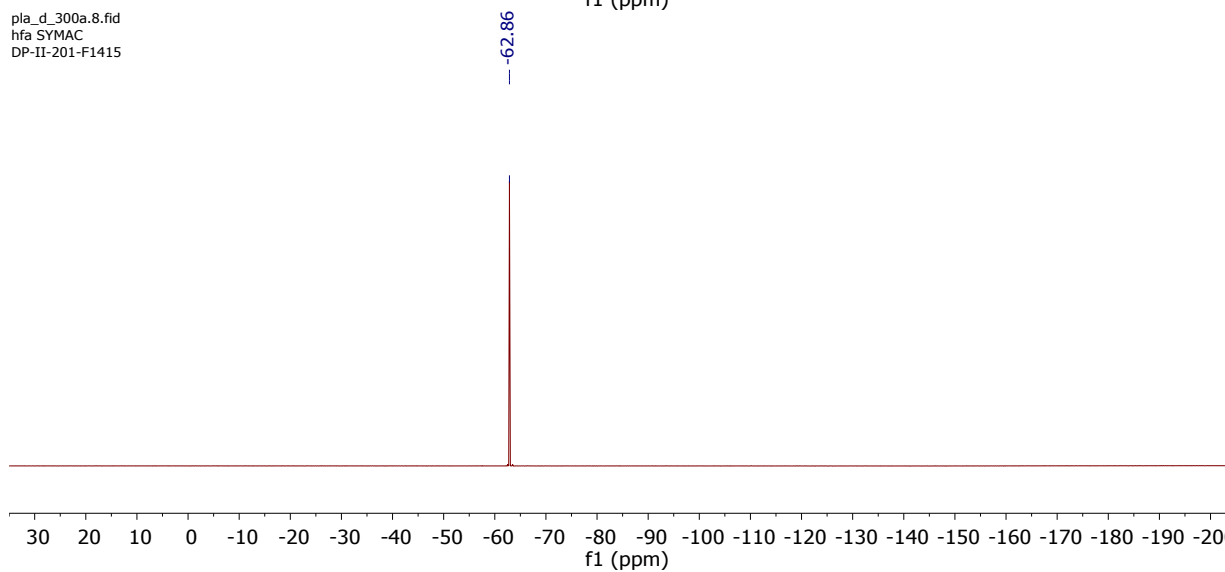
pla_d_300b.24.fid
hfa SYMAC
DP-II-201-F1415



pla_d_300b.26.fid
hfa SYMAC
DP-II-201-F1415



pla_d_300a.8.fid
hfa SYMAC
DP-II-201-F1415



K. References

1. A. Studer and D. P. Curran, *Nat. Chem.*, 2014, **6**, 765-773.
2. C. F. Nising, U. K. Schmid, M. Nieger and S. Bräse, *J. Org. Chem.*, 2004, **69**, 6830-6833.
3. N. Kirai and Y. Yamamoto, *Eur. J. Org. Chem.*, 2009, **2009**, 1864-1867.
4. A. R. Kapdi, G. Dhangar, J. L. Serrano, J. A. De Haro, P. Lozano and I. J. S. Fairlamb, *RSC Adv.*, 2014, **4**, 55305-55312.
5. L. Yang, T. Zeng, Q. Shuai, X. Guo and C.-J. Li, *Chem. Commun.*, 2011, **47**, 2161-2163.
6. G. Cahiez, C. Chaboche, F. Mahuteau-Betzer and M. Ahr, *Org. Lett.*, 2005, **7**, 1943-1946.
7. M. Kuroboshi, Y. Waki and H. Tanaka, *J. Org. Chem.*, 2003, **68**, 3938-3942.
8. J. Jin, M.-M. Cai and J.-X. Li, *Synlett*, 2009, **2009**, 2534-2538.
9. A. Moncomble, P. Le Floch and C. Gosmini, *Chem. Eur. J.*, 2009, **15**, 4770-4774.
10. J. Buter, D. Heijnen, C. Vila, V. Hornillos, E. Otten, M. Giannerini, A. J. Minnaard and B. L. Feringa, *Angew. Chem., Int. Ed.*, 2016, **55**, 3620-3624.
11. H. Tran, T. McCallum, M. Morin and L. Barriault, *Org. Lett.*, 2016, **18**, 4308-4311.
12. B. Kaboudin, T. Haruki and T. Yokomatsu, *Synthesis*, 2011, **2011**, 91-96.
13. J. Maddaluno and M. Durandetti, *Synlett*, 2015, **26**, 2385-2388.